

Periodic Windowed Behavior in SGR1935+2154 SGR Bursts

Bruce Grossan

UC Berkeley Space Sciences Laboratory, 7 Gauss Way, Berkeley, CA 94720, USA
Energetic Cosmos Laboratory, Nazarbayev University, 53 Kabanbay Batyr Ave., Block
C4, office 403, Nur-Sultan 010000, Kazakhstan
Bruce_Grossan@lbl.gov

Abstract

Two repeating FRB sources, FRB180916 (CHIME/FRB Collaboration, 2020) and FRB121102 (Rajwade, et al., 2020) display periodic windowed behavior (PWB) in the times of FRB detections. In PWB, events occur only within a periodic window spanning some fraction of the period, but additionally, in FRB121102, no events are detected at all during many of the periods. During 2020 May, coincident soft gamma bursts and fast radio bursts (FRBs) observed from SGR1935+2154 (Zhang, et al., 2020) established a clear link between at least some FRBs and soft gamma repeaters (SGR), and therefore magnetars. The analysis herein, which selects the period giving the minimum window fraction, shows PWB in this source's soft gamma-ray emission. For 174 bursts from 2014 through 2020 from IPN (Interplanetary Network) instruments, a clearly resolved minimum in window fraction vs. period occurs at a 231 day period, and 55% window fraction. Simulations show that PWB is not effectively identified by standard chi-squared methods used for pulsars. The data cover only 6 bursting episodes; discovery of events significantly outside the given windows could seriously change these conclusions. However, it is shown that this result is robust: First, the IPN has excellent time coverage and is unlikely to miss bursts outside of these windows. For several data sub-samples, the same period was found, and with large bursting episodes removed, the same period is among the best two or three. Simulations show that even small numbers of random bursts cannot show PWB; additionally, random events in the same number of periodic windows as the data yield errors in the period $\sim 1\%$ for even much smaller data sets. These checks show the results are not due limited sampling. The periodicity of this SGR's bursts should therefore provide critical hints as to the mechanism behind the bursts, and by association, FRBs.

1. Introduction

The year 2020 has been unprecedented in the study of transients, in that the number of cosmological FRB detections has exploded, and this previously believed extragalactic phenomenon was observed in a known galactic soft gamma-repeater, SGR1935+2154, with simultaneous soft gamma bursts (SGBs; Zhang, et al., 2020). There may be important caveats to the precise relation of the SGR1935 event and cosmological FRBs (e.g., Margalit, et. al. 2020), but the event proves that FRBs can be made by SGR (putatively magnetar) sources, and that FRBs may be accompanied by SGBs. The latter point raises the emission physics question, “what is the set of physical processes/events that results in both SGBs and FRBs?” There are many forms of inquiries that may be undertaken to shed light on this question. Attempting to measure the spectrum simultaneously from as much of radio to gamma-ray frequencies as possible would help make and test emission mechanism models. However, another surprising recent discovery gives a different mode of inquiry: periodic windowed behavior (PWB) of repeating FRBs.

In PWB, events are measured only within periodically recurring windows covering some fraction of the period, but many periods may have zero detected bursts. (Note, however, that whether the windows without bursts are 100 % burst-free is not truly known, since the sources have not been observed without interruption for the entire windows at high sensitivity thus far.) PWB have thus far been reported for two repeating FRB sources, that of FRB121102, $P \sim 157$ days and window fraction 56% (Rajwade, et al., 2020) with no detections during many periods, and in FRB180916, $P = 16.35$ days, $\sim 25\%$ activity cycle (CHIME/FRB Collaboration, 2020), with bursts reported in all cycles.

Behavior within a periodic window suggests that either some of the causal conditions for the behavior occur periodically, a “production” mechanism, or that conditions for observing the behavior occur periodically, i.e. a “shutter”/alignment mechanism. Most of the magnetars known have a measured pulsation period, believed to be the spin period of the neutron star. These are in the range of 2-12 s (Younes, et al., 2017) and are very far from the windowed periods reported.

SGR1935+2154 (aka SGR J1935+2154) was discovered in 2014 July (Stamatikos, 2014). Much of the information known about this source from observations up to 2016 are given in (Younes, et al. 2017). It has been detected by several X–gamma ray instruments and in radio. It is associated with the supernova remnant G57.2+0.8.

2. Data

2.1. Overview

SGR bursts are usually reported in the Gamma Coordinates Network (GCN) SGR Archive. Table 1 offers a summary of these reports. There appears to be a dichotomy of

episodes, those with many bursts over numerous days, of duration ~31-43 days, or those bursts detected on just one or two days. For shutter/align mechanisms (see Introduction), the much shorter or less numerous burst episodes cannot be dismissed or given substantially reduced weight. (For a more probabilistic view, it may be appropriate to weight bursting activity by episode duration, number of bursts per episode, etc.)

Table 1- Summary of Bursting Activity from the GCN Archive

Episode	Firstdetct	Lastdet	Center	Dur(d)	Summary
2014-07	2014-07-05	07-05	07-05	1	Single day activity BAT
2015-02to04	2015-02-22	04-12	03-15	43	A few BAT and 1 K-W burst
2015-12to 2016-02	2015-12-21	02-01	01-10	40	2 bursts, Integral, Fermi
2016-05to06	2016-05-18	06-25	06-05	41	12 K-W bursts
2019-10to11	2019-10-04	11-05	10-20	33	3 K-W, various BAT bursts
FRB2020- 04to05	2020-04-10	05-10	04-25	31	2 Simultaneous FRB+"forest of bursts"

Firstdetct = first incidence of detection in this episode; Lastdet = last GCN detection in this episode; Center = midway between first and last detections; Dur = Duration, in days. Note that the 2016-01 burst is apparently not explicitly given in the GCN archive, and in the K-W data it is only a one burst/one day episode.

2.2. Data Selections

In an ideal world, an instrument with uniform sensitivity to some burst criteria would continuously monitor a given source, and then analyzing all bursts, one could make a definite statement about periodicity or other behaviors within these parameters. In reality, there are many non-idealities to SGR data. A number of instruments operate with widely varying sensitivities, with many inherent periodicities including sensitivity, background, coverage duty cycle, etc. Further, if one instrument detects a bright burst, then other instruments with widely varying sensitivity will frequently schedule observations at some time soon after this, yielding bias toward clusters of bursts after a bright burst. Even this type of coverage is not uniform, however, due to observing constraints. At some level, particularly for faint bursts, the reporting of a burst in acquired data depends on the data reduction, mostly through the burst criteria (but also through background subtraction methods and other, sometimes model-dependent factors).

Many bursts between 2014 and 2016 are reported and analyzed in Younes, et al., 2017, and constitute burst episodes beginning 2014 July 05, 2015 Feb 22, and 2016 May 14, and 2016 June 18. Their displays of bursts vs. date (but not their full analysis) are from bursts detected by IPN (Interplanetary Network; Hurley, 2007) instruments, including the Konus instrument (10-770 keV) aboard the *Wind* spacecraft (K-W), stationed at L1. K-W provides a nearly continuous, unobstructed view of the entire sky, an excellent set of

properties for timeseries monitoring. The main downside to these data is that much more sensitive instruments exist, and weaker bursts are missed. If shutter/align phenomena are of primary interest, it may be more important to include all bursts than to have a uniform sensitivity. One cluster of bursts from K-W, on 2019 Nov 4 and 5 (Ridnaia, et al., 2019), was not reported by more sensitive wide-field instruments, including Fermi-GBM. This demonstrates the almost complete time coverage of this instrument, even though the collecting area is rather small. It also demonstrates the problem of sensitivity vs. coverage; if other instruments covered the event, they might have found many weaker bursts covering a much wider time window.

All confirmed bursts from the source detected by any spacecraft in the IPN (Interplanetary Network; including K-W, Fermi GBM, and Swift-BAT), through 2020 March, were obtained from the IPN website (Hurley, 2007). These data notably do not include the 2020 FRB episode.

To supplement the IPN data in 2020, these steps were followed for additional data :

- The GCN SGR circulars header list were searched for all mentions of the character string “1935”.
- Every detection of any kind of burst from SGR1935 above 1 keV was noted. K-W detections generally represented the activity detected, and so for uniformity, only K-W detections were used. Not all burst times were explicitly given, however, GCN 27631 on 2020 Apr. 21 gives 17 bursts in the episode. An earlier GCN explicitly gave one burst on Apr. 10, so the remaining 16 were therefore distributed approximately evenly from Apr. 11-21 for our analysis.
- A “Forest of Bursts” was reported in GCNs for 2020-04-28 (Palmer & BAT Team, 2020), up to 35 bursts (Swift-BAT) in a period of a few hours, and this cluster of bursts appears to be among the most numerous of all from SGR1935+2154. This is much larger than the number of bursts on any other day. The K-W team reported “several tens of bursts” in a short period (Ridnaia, et al., 2020a). Thirty bursts were therefore added to our data on this date for our analysis, an approximate number.

The following data selections were analyzed:

IPN Plus (IPN+) – All IPN bursts to 2020 March plus the K-W bursts reported in GCNs as given above.

K-W Only (KWO) – Only the K-W bursts given in the GCNs.

Unrestricted Equal Weight Episodes- (UEW) The average long episode duration, 37 days was used, and the same number of bursts were distributed over 37 days around the center of all 6 episodes. (This is an artificially constructed data set intended to explore the concept of a periodic shutter mechanism modulating random events.)

We offer two additional samples in order to test the sensitivity of our result to removing a single large burst episode. **IPNA** is the IPN+ selection with the mid-2016 episode, our richest episode, with the largest number of days with bursts, removed. **IPNB** is the IPN+ selection with the 2020 episode removed.

3. Methods: Analysis of Periodic Windowed Behavior

Periodic behavior, especially in pulsar studies, typically uses Fourier analysis, or Lomb-Scargle Periodograms. These can give poor results for sparsely and unevenly sampled data, and all the more so for not truly periodic behavior. Folding data into finite “phase” bins has been used in many contexts, and various methods are used to determine the best period, such as maximizing the chi-squared, (that is, the sum of the data minus the global average among the phase bins, squared, divided by sigma squared) and the minimum string length method. These methods are not optimum for this task (e.g. the chi-squared maximization will favor a narrow peak, though it’s not clear such a peak would be the correct answer) and were not used.

As we are looking for windowed periodic behavior, the folded profile periods were evaluated by the smallest window that would contain 100% of the data, or w100, expressed as the fraction of the period covered by the window. This statistic is calculated without regard to the peak profile, i.e. it is not symmetric about the folded profile peak. The data were folded at a range of trial periods in single day steps and 10 phase bins for our profile plots (the chi-squared statistic is not used for any selection here, but it is calculated for this binning). Both the minimum w100 widths and the presence of any obvious “dip structure” in the w100 vs. period plot were noted. Three of the four burst episodes occur within about 800 days, therefore, period durations were searched between about 100 and 400 days.

4. Results

4.1. Event Analysis

The results of period folding and w100 measurements are summarized in Table 2. Figs 1-3 show the w100 vs. period plots for some of the data selections. **Figure 1** shows, for the IPN Plus data selection, the largest data set, that a minimum of w100, 55%, occurs near the center of a resolved, smooth dip, at a period of 231 days; **this 231 day period therefore best describes the PWB in the SGBs**. The center of the dip is approximately 3 days away from the minimum, indicating that by this measure, the uncertainty is ~ a few days, or less than 2% of the period. Figure 4 shows the data and derived periodic windows.

For the IPN A selection, with the episode with the most burst days removed, the minimum w100s was not at the 231 day period, but at 268 days. However, the 231 day period is the center of the second lowest dip in w100, not significantly deeper (48% vs. 45%). The IPN B selection with the 2020 episode removed has the preferred 231 day period for the

w100 minimum. In the K-W Only data selection, dips are present at 204, 141, and 238 days, the latter very close to the preferred 231 day period.

Table 2 Samples, Trial Periods, and 100% Width

Sample	Period(d)	W100	Chi-sq
*IPN+	231	0.554112	197.189
IPN+	232	0.556034	252.4
IPN+	233	0.55794	222.332
IPN+(c)	234	0.559829	290.681
IPN+	235	0.561702	274.732
*IPN+	277	0.628159	186.493
(c)IPN+	280	0.632143	271.569
*(c)IPN+	393	0.640585	184.942
*IPNA	268	0.45056	135.702
IPNA	269	0.452602	181.149
IPNA	270	0.45463	174.003
IPNA	271	0.456642	147.766
(c)IPNA	272	0.45864	140.46
*IPNA	233	0.477468	122.454
(c)IPNA	231	0.495671	110.068
*(c)IPNA	153	0.50817	70.2602
*IPNB	231	0.554112	148.019
IPNB	232	0.556034	143.512
IPNB	233	0.55794	154.388
IPNB	234	0.559829	174.681
IPNB	235	0.561702	172.504
(c)IPNB	239	0.569038	165.691
*IPNB	277	0.628159	145.319
(c)IPNB	282	0.634752	145.628
*(c)IPNB	392	0.637117	162.621
*(c)KWO	204	0.229167	29.1633
KWO	203	0.235222	22.5499
KWO	205	0.24878	29.1633
KWO	202	0.266089	22.9456
KWO	206	0.281553	24.4643
*(c)KWO	141	0.335106	22.867
*(c)KWO	238	0.339286	23.3345
*(c)UEW	235	0.52766	236.06
UEW	236	0.529661	244.12
UEW	234	0.530983	219.505
UEW	237	0.531646	262.626
*(c)UEW	175	0.532857	215.324
*UEW	317	0.593849	231.401
(c)UEW	314	0.609076	219.094

The table above lists the lowest 5 w100 values for each data selection, plus the approximate center (c) and minimum (*) values of the next two lowest resolved dips in w100. Note the dip center and minimum can be the same.

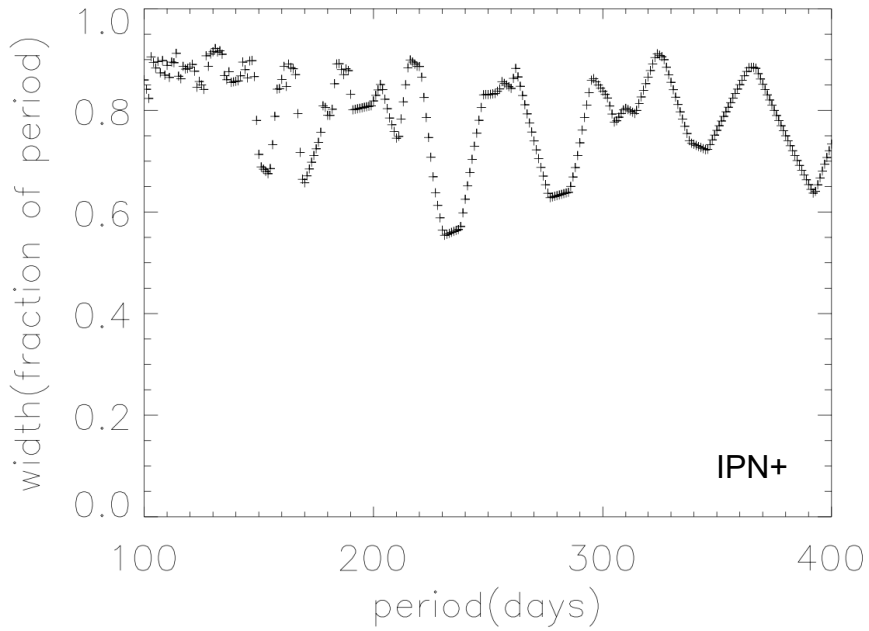


Figure 1 Periodic Window Fractional Width (W100) vs. Period for the IPN+ Selection. The minimum w_{100} , or the width of a periodic window containing 100% of the data, gives the preferred 231 day period from this, the largest data set.

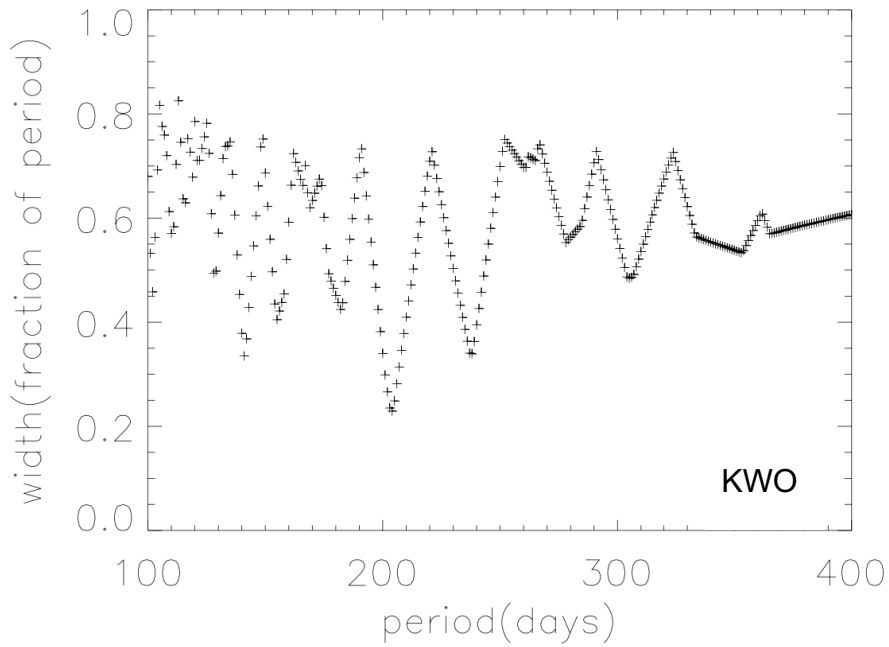


Figure 2 W100 vs. Period for the KWO selection. The deepest minimum is at 204 days, but another is present at 238 days, near the nominal period. This data sample is much smaller than the previous.

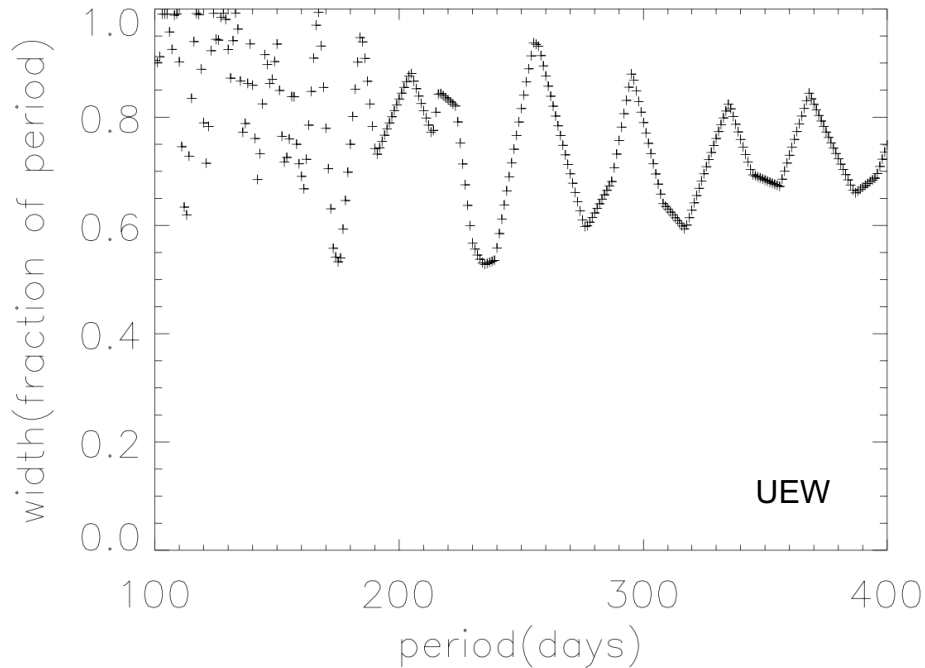


Figure 3 W_{100} vs. Fold Period for the UEW selection. There is a prominent dip at 232-240 days, also near the w_{100} minimum value for the IPN Plus selection.

The folded data give a “pluse profile”, shown in *Figure 5* for the IPN Plus data selection. (Two cycles are shown, following standard astronomical convention.) This profile is not like a pulsar pulse profile or other periodic behavior profile, as the behavior is not known to be strictly periodic; it should not suggest there is a clear burst probability vs. phase function, either. There are simply not enough data within each window (just two points in some episodes) to draw a significant conclusion about structure within the window. The profile could change with future data, even if such data are consistent with the activity windows we find here. The profile does show a peak, however. This peak is at the same phase in all analyses at the 231 day period (and in the minimum W_{100} period for IPNB), except in the UEW sample, which is expected to remove profile structure. Note that the UEW selection still yields almost the same resulting W_{100} minimum period as the IPN Plus selection (*Figure 6*).

5. Simulations

5.1. Random Data

The analysis of random data with similar general characteristics to the actual data helps assess the veracity of the result. The random data were reduced with the same software as the real data. Many realizations of simulated data sets were made and analyzed, with events distributed at random (uniformly) over 2400 days, about the same time span from the first to the last burst. Analysis of these simulated event streams shows that the larger the number of burst events, the less likely small w_{100} values will be produced, i.e. the

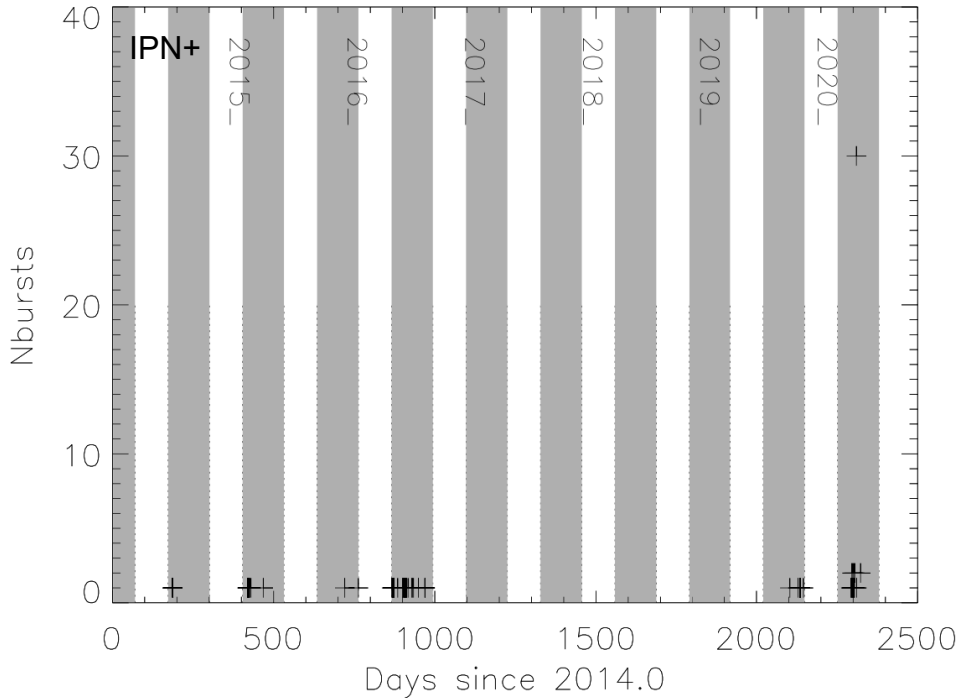


Figure 4 IPN+ selection bursts and windows. The figure shows the IPN Plus data selection folded at the 231 period of minimum W100, 55%. The Data Selections are described in Section 2.2.

less likely significant PWB will be found. The probability of $W100 \leq 56\%$ is $\sim 4 \times 10^{-5}$ for 32 events. The probability of a false periodicity and similar W100 for 174 events, the same number as in the IPN Plus sample, is vanishingly small, and could not be determined with only the $\sim 10^5$ trials used here.

5.2. Periodically Windowed Random Data

Assume the hypothesis that the true phenomenon is random events that either only occur, or are only observable, during some of the periods, and only within periodic windows. In this case, analysis of simulated data can demonstrate the limitations of measurement of PWB periods and w100. In particular, one might anticipate that with small numbers of events, it would be difficult to determine the period or window fraction. Random (uniformly) distributed events were therefore generated with the same characteristics as the real data, i.e. near the claimed 231 day period and 55% window fraction, and activity in only 6 of 11 periods. Sets of such randomly generated data, with different numbers of total data points, were therefore generated to assess the quality of the results of our analysis.

The period determination turned out to be very good as long as more than about 43 events were in the data set (fractional variation of \sim percent; *Figure 7*). With only a few times 10^3 realizations and 43 events, we could not find any instance of the W100 method more than a few percent off the true period. The W100 value itself, however, showed significant variation (always underestimating) until about 100 points, where the errors were $< 5\%$ (*Figure 8*). This can be understood by imagining starting with a data set with good, uniform coverage, then removing points at random one-by-one. Eventually, the extrema points of each window would be removed, and the W100 would decrease. However, the period

would still be present in the data. (The folded profile, a square wave with large numbers of points, would lose non-zero values from more phase bins as the number of points was reduced.)

Random windowed data were also reduced by chi-square maximization. Period values with very large (~50%) errors were present for 86 points (compare to a clear convergence and less than 5% errors for 43 events with w100 minimization). For window fractions, the w100 method gave errors < 10% at 129 events; chi-squared method errors did not continue to decrease after 43 events, and errors never became small. This reduction clearly demonstrates that the chi-squared technique does not work well for PWB, though regularly used for true periodic behavior.

6. Discussion

6.1. Robustness of Results

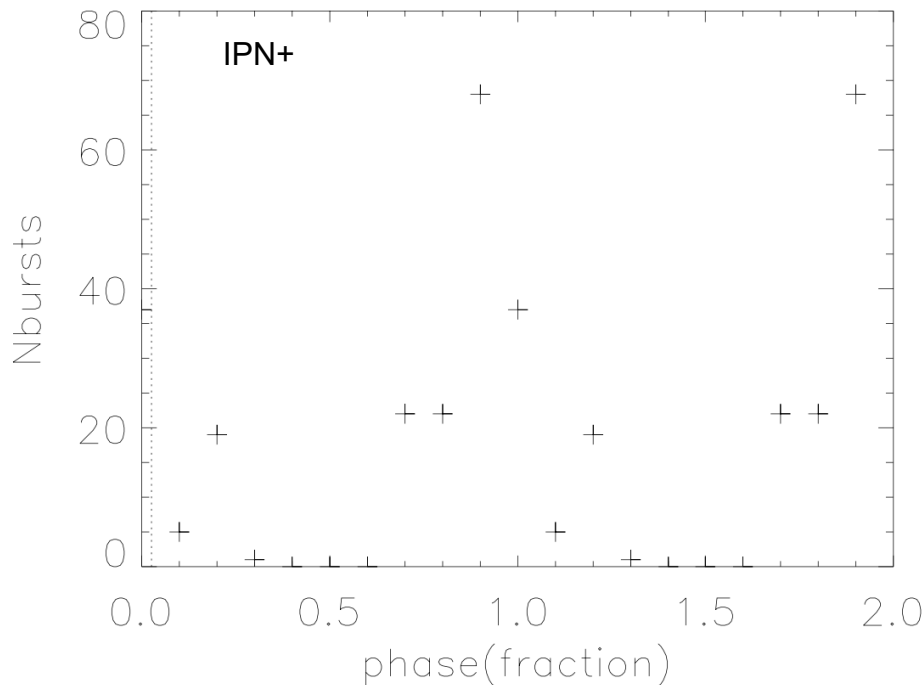


Figure 5 Folded profile at 232 day period. IPN plus selection. (Note profile is repeated twice, following astronomical convention).

The data cover only six bursting episodes; one consists of only two burst detections, and another covers only one day. A single future episode of many bursts badly out of phase with our preferred PWB parameters would significantly change our results. Therefore, we cannot say with certainty that the observed PWB could not be overturned by later observations. However, several points give us confidence that little will change with re-analysis or additional data in the epochs we cover: First, de-selecting significant amounts of the data often had little effect on the results. Removal of even the richest episode, i.e. removal of the episode with the largest number of days with bursts, the IPN A selection,

yielded essentially consistent results: though the preferred period was the minimum of the second lowest dip in w_{100} , not the lowest, it was nearly as deep, 48% vs. 45%. Removal of the rich 2020 episode, the IPN B selection, yielded the preferred period. Next, it is unlikely that, down to the sensitivity of K-W, any bursts have been missed between the given windows. Where required for localization, the IPN also includes the ensemble coverage of Fermi GBM (all-sky, but with earth occultation; NASA, 2011), BAT (~2.2 Sr; Barthelmy, 2004), and others. The time that no other instruments would be covering SGR1935 to yield a consistent localization, when combined with K-W, is small. Finally, the random simulations show that any $w_{100} \leq$ our nominal is very unlikely unless ~32 events or less are used. This means that the skeptic may eliminate any of our data for any type of test or different analysis, but unless the data are reduced by a factor of ~5, random data are extremely unlikely to produce a W_{100} as small. Finally, if we assume the hypothesis of windowed periodic behavior is correct, and events are distributed uniformly with the active windows, the number of data points available suggest errors on our W_{100} and period values of less than a few percent. Taken together, these points suggest a robust result.

6.2. The Origin of Windowed Periodicity

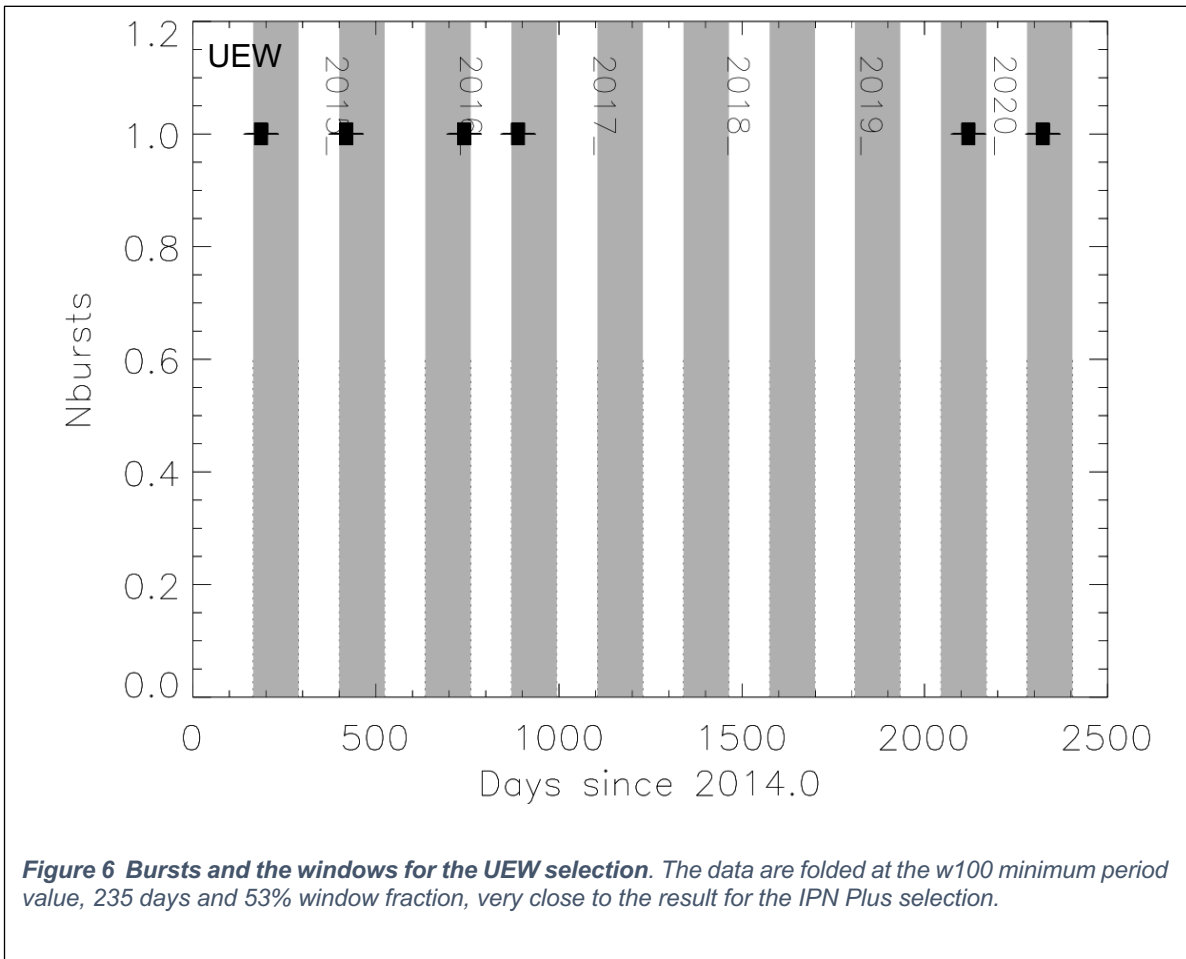


Figure 6 Bursts and the windows for the UEW selection. The data are folded at the w_{100} minimum period value, 235 days and 53% window fraction, very close to the result for the IPN Plus selection.

Windowed periodicity, as observed here and in repeating FRBs, is not as yet associated with a physical mechanism. At first glance, one might wonder if the influence of an orbital companion might produce the periodic behavior. Magnetars are almost by definition isolated neutron stars (NS) powered by magnetic energy (e.g. Mereghetti, 2008) and have distinct properties from X-ray binaries. No accretion activity is proposed for SGRs, unlike X-ray binaries. There are FRB models that have a companion and no accretion (Zhang & Gao, 2020, and references therein), including the Binary Comb Model (Ioka & Zhang, 2020), though no confirmed magnetar companions are known. The latter model produces FRBs in the interaction of a B star wind and a NS. In using this model to explain the ~ 16 day periodicity in rFRB180916 (Zhang & Gao, 2020), it was found that binaries with periods from 1-100 days would form, but “after 100 days the birth rate significantly decays”. As the periods for SGR1935-2154 SGBs, and for rFRB121102 FRBs are significantly larger than 100 days, either the model needs modification or it does not explain these objects.

Models explicitly addressing simultaneous FRB/SGR events may invoke pair production involved in the SGBs (generally believed to originate in crust disturbances) and a magnetospheric interaction to produce the FRB relatively nearby the surface (Kumar &

Bošnjak 2020; Kumar et. al. 2017), or e.g. a jet and shock model, that emits the radio burst relatively farther from the NS surface (Margalit, et. al. 2020). These models do not explicitly consider periodicity or a companion, however. A periodic phenomenon might modulate the orientation or structure of the magnetic field affecting magnetospheric phenomenon or jet containment. A mechanism for affecting the magnetic field might be some motion of an accretion disk, as ionized matter can drag field lines. Early discussions of SGR activity proposed some kind of accretion disk, possibly a remnant (e.g. Mereghetti, 2008). Though the Keplerian periods of objects near a NS are far shorter than 231 days, it is conceivable that this periodicity could be some kind of “beat frequency” with another period, e.g. an orbital period and some period of disk motion that are close, but not matching. There is, however, no evidence of any such disk, and early relic accretion disk models for SGRs are no longer favored (i.e. not mentioned in the recent references herein).

Another origin of periodicity is in regulation of the visibility of emission, a “shutter” or alignment mechanism, rather than in the emission itself. How a periodic phenomenon might produce conditions favorable for viewing soft gamma and fast radio bursts, or periodically remove an obscuration to favor observation, is not obvious. Note that to obscure gamma-rays a substantial column of gas or electrons would be required.

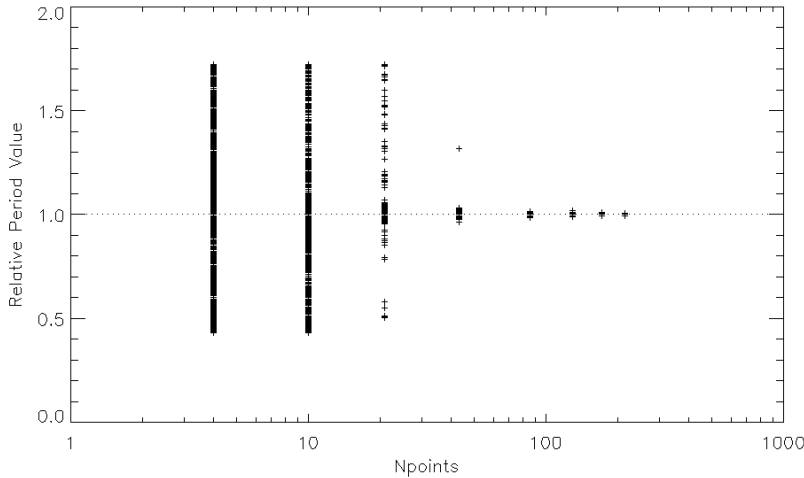


Figure 7a. Measured period values from random events in periodic windows. At 43 events or more, the correct period is determined with $<1\%$ error; at 86 events no outliers are found. (The apparent small number of points at large N_{points} is due to integer period values; 2500 realizations were made for each N_{points} value.)

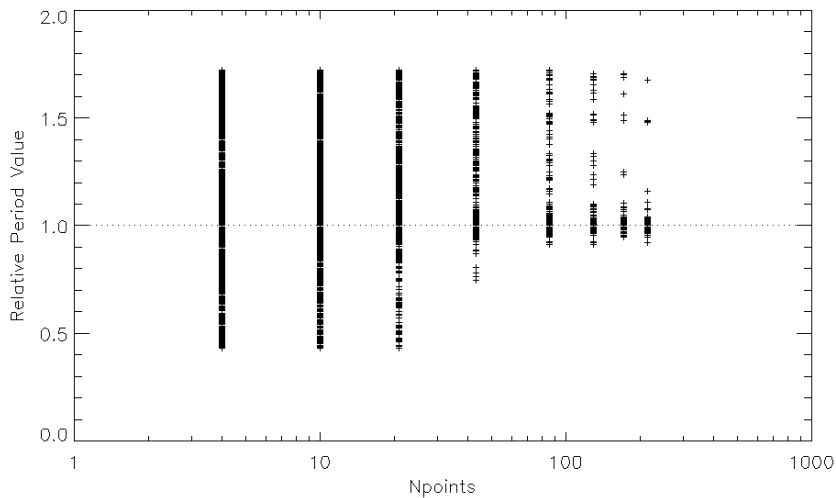


Figure 7b. Measured period values from random events in periodic windows by chi-squared maximization method. The variance in the period is much larger than for the w100 method, and even for 215 data points, there are still alarming outlier results. The same number, 2500 realizations were made.

7. Conclusion

A folding analysis was used to show PWB in the broadly defined SGBs of SGR1935-2154. It is extremely unlikely that this result would come from insufficient or irregular sampling of uniform random data. It was also shown that for simple assumed PWB, random events with the given period and window fraction PWB, the number of bursts makes it unlikely that the period or window fraction could be far off the correct result. Though the PWB result appears robust, no identification with any known mechanism for the PWB was found. It was also shown, however, that a conventional chi-squared

analysis is poor at identifying PWB. It could be that PWB is not uncommon, but rarely recognized thus far. Further identification of PWB in various emissions from stellar systems may help identify the physical mechanism causing it.

This work in no way addressed burst characteristics such as duration or fluence, nor spectral properties. These are likely physically important, e.g., in GCN 27669 reporting the detection of a burst coincident with an FRB (Ridnaia, et al., 2020b), this observation was offered: “The burst temporal structure and hardness differ from a typical SGR burst ... suggesting a possibly different emission mechanism.” Perhaps only a tiny subset of the bursts studied here are associated with the actual physical mechanism of FRBs. However, given that PWB is common to the one known galactic FRB source and several repeating extragalactic FRB sources, PWB is likely a general characteristic of FRB-causing systems. This characteristic can then be a required feature of future models of magnetars and FRBs, serving to restrict the variety of possible models, and steer us toward a proper identification of the as yet mysterious physical mechanisms behind FRBs.

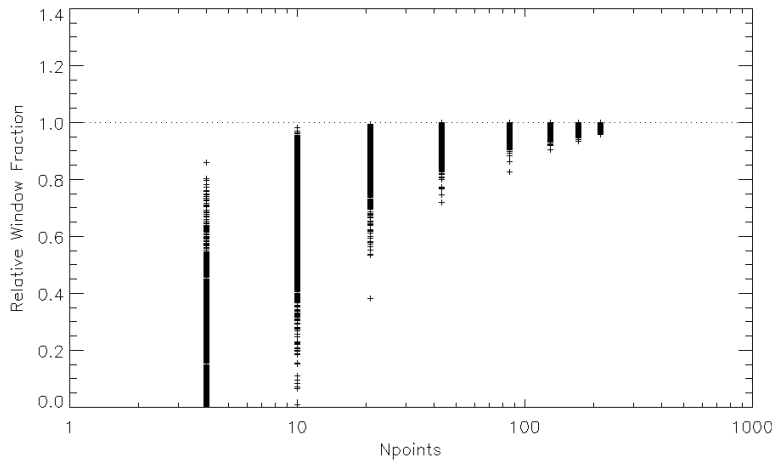


Figure 8a Measured window fraction from random events in periodic windows, by $w100_{\min}$. The standard deviation in the minimum window fraction is less than 4% with 43 points (but biased low). Each N_{points} is 2500 realizations.

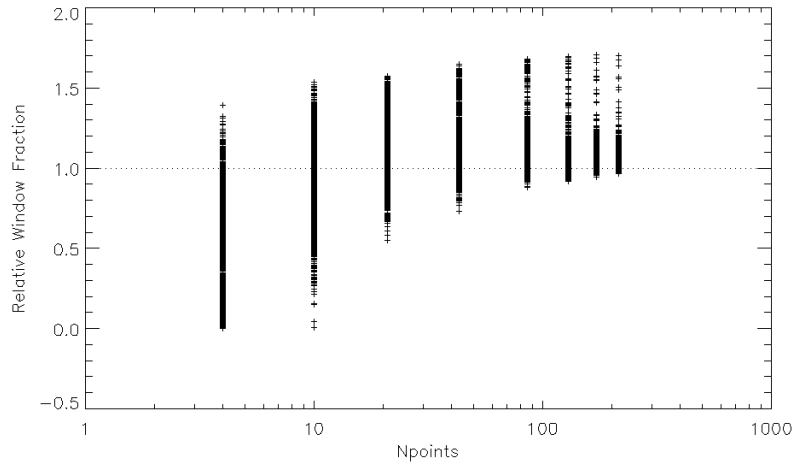


Figure 8b. Measured window fraction from random data, by chi-square max method. Even above 200 points, the errors are large and outliers remain. Also 2500 realizations for each N_{points} .

Acknowledgments

I thank Eric Linder and Kevin Hurley for valuable discussions, and the staff and scientists of the Energetic Cosmos Laboratory for support in this work. This paper has made use of data at the IPN website, ssl.berkeley.edu/ipn3, maintained by Kevin Hurley.

8. Works Cited

- Barthelmy, S. D. (2004). The Burst Alert Telescope (BAT) on the Swift Midex Mission. *Proc. SPIE*, 5165.
- CHIME/FRB Collaboration, T. (2020). Periodic activity from a fast radio burst source. *Nature*, 582, 351.

Hurley, K. (2007, July). Retrieved from The Third Interplanetary Network:
<http://www.ssl.berkeley.edu/ipn3/>

Ioka, K., & Zhang, B. (2020). *ApJL*, 893, L26.

Kumar, P., & Bošnjak, Ž. (2020). *MNRAS*, 494, 2385.

Kumar, P., Lu, W., & Bhattacharya, M. (2017). *MNRAS*, 468, 2726.

Margalit, B., Beniamini, P., Sridhar, N., & Metzger, B. D. (2020). *arxiv.org*, 2005.05283.

Mereghetti, S. (2008). *A&A Rev.*, 15, 225.

NASA. (2011). *Fermi Gamma-Ray Telescope*. Retrieved from
<https://fermi.gsfc.nasa.gov/science/instruments/table1-2.html>

Palmer, D. M., & BAT Team. (2020). *GCN*, 27665.

Rajwade, K. M., Mickaliger, M. B., Stappers, B. W., Morello, V., Agarwal, D., Bassa, C. G., . . . Lorimer, D. R. (2020). *MNRAS*, 495(4), 3551.

Ridnaia, A., Golenetskii, S., Aptekar, R., Frederiks, D., Ulanov, M., Svinkin, D., . . . Konus-Wind Team. (2020a). 27667.

Ridnaia, A., Golenetskii, S., Aptekar, R., Frederiks, D., Ulanov, M., Svinkin, D., . . . Team, K.-W. (2019). *GCN*, 26242.

Ridnaia, A., Golenetskii, S., Aptekar, R., Frederiks, D., Ulanov, M., Svinkin, D., . . . Team, K.-W. (2020b). 27669.

Stamatikos, M. M. (2014). SGR1935+2154 discovery announcement. *GCN*, 16520, 1.

van Kerkwijk, M. H. (1995). *ApJL*, 444, 33.

Younes, G. K. (2017). *ApJ*, 847, 845.

Zhang, S.-N., S.-L., X., C.-K., L., X.-B., L., Y.-L., T., Ge M.-Y., Z. X.-F.-M.-Y.-S.-C.-J.-M., . . . Cao X.-L., X. Y.-P.-P. (2020). *GCN*, 27675.

Zhang, X., & Gao, H. (2020). *MNRAS*, slaa116.